Comparison of the Satellite Attitude Control System Design Using the H∞ method and H∞/MLI with Pole Allocation Considering the Parametric Uncertainty

ALAIN G DE SOUZA
ITA, Technological Institute of Aeronautics,
São José dos Campos, São Paulo, BRAZIL

LUIZ C G DE SOUZA
UFABC, Federal University of ABC
Santo André, São Paulo, BRAZIL

Abstract: This paper presents the comparison of the Attitude Control System (ACS) design for a rigid-flexible satellite with two vibrations mode, using the traditional H∞ method and the H∞/LMI with pole allocation considering the parametric uncertainty. In the ACS design is important take into account the influence of the structure's flexibility, since they can interact with the satellite rigid motion, mainly, during translational and/or rotational manoeuvrer, damaging the ACS. Usually the mathematics model obtained from the linearization and/or reduction of the rigid flexible model loses information about the flexible dynamical behaviour and introduces some uncertainty. The satellite model is represented by a flexible beam connected to a central rigid hub considering a set of parametric uncertainties. Simulations results have shown that the control law designed by the H∞/LMI method has better performance and it is more robust than H∞ method since the first was able to support the action of the uncertainty perturbation and to control the rigid flexible satellite attitude and suppressing vibrations.

Key-Words: H∞ method, H∞/LMI, ACS, Parametric uncertainty, Flexibility, Satellite

1 Introduction

Satellites are design with specific functions and for accomplish them; the system need be able to execute some manoeuvrers around his center of mass (attitude manoeuvrers) [1]. These functions are: turning the solar panels facing the sun, stabilize the satellite after the orbital acquisition, point the cameras and/or sensors to the Earth or other planet, moon and star [2]. For conducting this kind of manoeuvrer is necessary have a lot of sensors and actuators with a good accuracy and precision. With that, for managerial all that, one need design a control system called attitude control system (ACS).

The flexible appendages play an important role in the satellites ACS performance, one example of this flexible appendages are the solar arrays [3]. Thus the dynamic of these flexible structures have to be included in the ACS design in order to investigate how its vibrational motion can affects the satellite rigid motion [4] during translational and/or rotational manoeuvrer which can result in damaging the ACS pointing accuracy [5].

Another problem is to recovery the loss of the dynamics information associated with the inability to obtain the real model, since the model reduction [7] can introduced some kind of perturbation which can be represented by the parametric and non parametric uncertainties where the first is associated with the parameters variation and the second with the unmodelled dynamics (unstructured uncertainty).

Than to obtain a ACS one applies the H∞ control method, since this method has the property to incorporate the uncertainties in its formulation [8] [9], and suppress the loss of the dynamics information, for example weak non linearities. Other technique used is the H∞ control method subject a pole allocation using Linear Matrix Inequalities (LMI). The main advantage of use the addition of LMI in the H∞ formulation is the possibility of make an pole-assignment in a determinate region defined by design, what does increase the sensibility of control [10].

The ACS design consider a model of a satellite with one panel, like the China Brazil Earth Resources Satellite – CBERS fig.1, making an attitude acquisition around the axis here the system are more flexible, this kind of manoeuvrer can be modelled [11], by an analogous as a flexible rotatory beam.

The main point of the paper consists in study comparatively the performance and robustness of the H∞ method with the technique that join the H∞ method with a LMI pole allocation applied to a flexible satellite, considering parametrical uncertainty associate to the mass matrix. Those studies led to development of software capable of check the performance of de ACS design with a H∞ or H∞ with a LMI pole allocation subjects some requirements for select the best

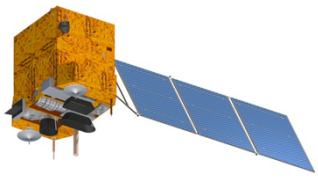

Figure 1: China Brazil Earth Resources Satellite – CBERS

controller, for a phase A of a project.

2 Robust controller design

For this problem it was design two controls law, one using a H∞ control method and other using the technique H∞ method with LMI pole allocation. The procedures used for this design are developed in sequence.

2.1 H∞ control method with parametric uncertainty

The H infinity control method have the advantage to inserts structured uncertainty and/or unstructured uncertainty in the design of the controller [12]. The philosophy behind this control method is found a gain $K_{H\infty}$ that minimizing the H infinity norm of the closed loop function (eq.1) in a system represented by a generalized plant model P,

$$F_l(P, K_{H\infty})\omega = P_{11} + P_{12}K_{H\infty}(I - P_{22}K_{H\infty})^{-1}P_{21} \tag{1}$$

$$\|F_l(P, K_{H\infty})\|_\infty = \max_\omega \bar{\sigma}(F_l(P, K_{H\infty})(j\omega)) \tag{2}$$

$$\|F_l(P, K_{H\infty})\|_\infty < \gamma \tag{3}$$

where $F_l(P, K_{H\infty})$ is the linear fractional transformation (LFT) of P and $K_H\infty$, and the γ is a design parameter which the smallest value is associated with the space state realization, such that the Hamiltonian H (eq.4), in a iteration process, has no eigenvalues on the imaginary axis [13],

$$H = \begin{pmatrix} A + BR^{-1}D^TC & BR^{-1}B^T \\ -C^T(I + DR^{-1}D^T)C & (A + BR^{-1}D^TC)^T \end{pmatrix} \tag{4}$$

where A, B, C and **D** are the space state matrices and $R = \gamma^2 I - D^T D$.

One can also include in the H-infinity solution some weight functions in the system as showed in the Fig. 2, in a sense to improve robustness, performance and stability.

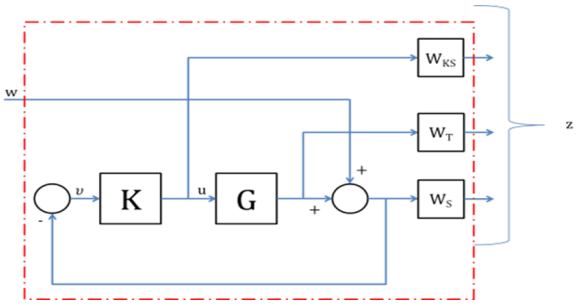

Figure 2: Tuning weight functions.

Should be mentioned that in the optimization of the H infinity control method to find the gain K one uses the criterion of the smallest value of γ associated with the tuning weight function which have the following form [9].

$$\begin{aligned} W_s &= \frac{s/M + \omega_b}{s + \omega_b A} \\ W_T &= \frac{s + \omega_{bc}/M}{As + \omega_{bc}} \\ W_{KS} &= \text{cte} \end{aligned} \tag{5}$$

The parameters of the weight functions are: A is correlated with the steady state, ω_b is the desired bandwidth of the sensitivity function, M is correlated with the overshoot, ω_{bc} is the desired bandwidth of the complementary sensitivity function [12].

2.2 H$_\infty$ method using a LMI pole allocation

For the pole allocation is necessary that the closed loop function obey the restriction $T_{wz\infty} < \gamma$ and the matrix X_∞ exists and $\mathbf{X}_\infty > 0$ [14].

$$\begin{pmatrix} V_{11} & V_{12} & V_{13} \\ V_{21} & V_{22} & V_{23} \\ V_{31} & V_{32} & V_{33} \end{pmatrix} < 0 \tag{6}$$

$$\begin{aligned} V_{11} &= (A + B_2K)X_\infty + X_\infty(A + B_2K)^T \\ V_{12} &= B_1 \\ V_{13} &= X_\infty(C_1 + D_{12}K)^T \\ V_{21} &= B_1^T \\ V_{22} &= -1 \\ V_{23} &= D_{11}^T \\ V_{31} &= (C_1 + D_{12}K)X_\infty \\ V_{32} &= D_{11} \\ V_{33} &= -\gamma^2 I \end{aligned} \tag{7}$$

To guarantee the pole allocation in a LMI region defined by,

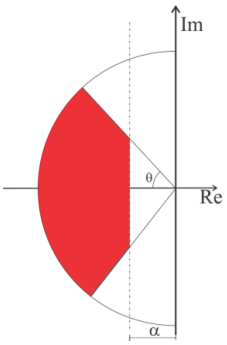

Figure 3: LMI Region

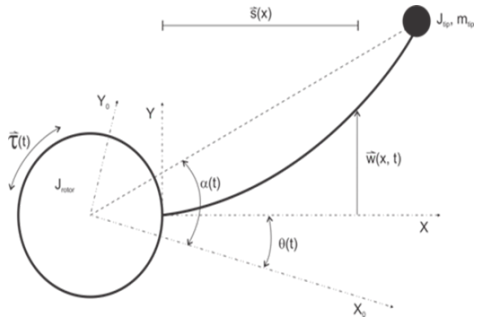

Figure 4: Satellite Analogous Representation

$$D = \left\{ z \in C : L + zM + \bar{z}M^T < 0 \right\} \quad (8)$$

with $L = L^T = [\lambda_{ij}]_{(1\leq i,j\leq m)}$ and $M = M^T = [\mu_{ij}]_{(1\leq i,j\leq m)}$. And is necessary, there is a matrix $X_{pol} > 0$ that satisfies the relationship:

$$\lambda_{ij}X_{pol} + \mu_{ij}(A + B_2K)X_{pol} + \mu_{ij}X_{pol} + \mu_{ij}X_{pol}(A + B_2K)^T_{1\leq i,\, j\leq m} < 0 \quad (9)$$

That conjunct of conditions is create a non-convex optimization with the variables K, X_∞ and X_{pol}.

Then for the case in study the pole allocation it's chosen the combination of three LMI regions, a plan, a half disc and a conic sector [10] this region is represented by the Fig.3.

The intersection of these three regions guarantees an allocation of poles such that the transient response is: 1) decay rate equal α; 2) Natural frequency of minimum damping $\zeta = \cos(\theta)$; 3) Natural frequency undamped $D = r\sin(\theta)$. This turn the limits of the maximum overshoot, the frequency of vibration modes, the delay time, rise time and duration of the accommodation. Thus, the pole assignment in the closed loop system, in that region, provides a satisfactory transient response.

3 Dynamic model with parametric uncertain

The rigid-flexible satellite was modelled like an analogues system composed by a flexible rotatory beam [6]. The actuator is located in the central part, and it is responsible for the control of the horizontal planar movement of the rigid structure and by the elastic displacement, where (X_0, Y_0) and (X, Y) are the coordinates system before and after deformation, respectively. The rigid central hub has radius R, the actuator rotor has viscous friction b_m, and inertia J_{ROTOR} and develops a torque $\tau(t)$; the flexible beam has uniform linear mass density ρ, uniform bending stiffness EI and length L; the flexible beam deformation is $w(x, t)$; and the tip mass is m_{tip} and inertia J_{tip}; $\alpha(t)$ represent the tip angle and $\theta(t)$ is the rigid angle displacement; and $s(x)$ represent the distance between the referential axis to an element of mass in the link.

The flexible link is considered an Euler-Bernoulli beam.

The equations of motion are derived using the Lagrangian approach combined with the assumed modes method, admitting two vibrations mode. Like show in [5] the equations of motion was derived using a Lagrangian approach combined with the assumed modes methods, admitting two vibrations modes and a dissipation of energy in a Rayleigh form [5]. Then the equations linearized of the dynamics are represented in a matrix form:

$$\begin{pmatrix} I_t & M_{rf}^T \\ M_{rf} & M_{ff} \end{pmatrix} \begin{pmatrix} \ddot{\theta} \\ \ddot{q} \end{pmatrix} + \begin{pmatrix} b_m & 0 \\ 0 & B_{ff} \end{pmatrix} \begin{pmatrix} \dot{\theta} \\ \dot{q} \end{pmatrix} + \begin{pmatrix} 0 & 0 \\ 0 & K_{ff} \end{pmatrix} \begin{pmatrix} \theta \\ q \end{pmatrix} = \begin{pmatrix} \tau \\ 0 \end{pmatrix} \quad (10)$$

With,

$$B_{ff} = k_e EI \int_0^L \varphi'' \varphi''^T dx$$

$$K_{ff} = EI \int_0^L \varphi'' \varphi''^T dx$$

$$M_{ff} = \rho \int_0^L \varphi\varphi^T + m_{tip}\varphi_L\varphi_L^T + \frac{1}{2}J_{tip}\varphi'_L\varphi'^T_L$$

where θ is the rigid angular displacement, q the flexible displacement vector and φ is the function of the modal form. By analogies, the Eq.**??** represent the standard form $M\ddot{x} + D\dot{x} + kx = Qu$, where the matrix are called M is the mass matrix, D is the damping matrix and K is the rigid matrix. Writing the space state form,

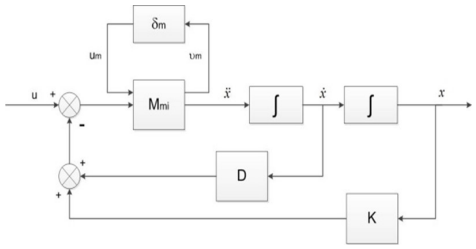

Figure 5: Block diagram of the system with uncertainty

$$\begin{pmatrix}\dot{X}_1\\ \dot{X}_2\end{pmatrix} = \begin{pmatrix}0 & I\\ -M^{-1}K & -M^{-1}D\end{pmatrix}\begin{pmatrix}X_1\\ X_2\end{pmatrix} + \begin{pmatrix}0\\ M^{-1}q\end{pmatrix}u \quad (11)$$

with $X_1 = \theta$ and $X_2 = q = (q_1 \;\; q_2)$ is the state's vectors and the control $u = -K_{(}H\infty)X$, where $K_{H\infty}$ is the gain calculate by the H infinity method.

3.1 Uncertainty design

The uncertainty of the mass matrix (M) can be introduced re-writing Eq.11 in the follow form:

$$\begin{pmatrix}\dot{X}_1\\ \dot{X}_2\end{pmatrix} = \begin{pmatrix}0 & I\\ M_{inc}K & M_{inc}D\end{pmatrix}\begin{pmatrix}X_1\\ X_2\end{pmatrix} + \begin{pmatrix}0\\ M_{inc}Q\end{pmatrix}u \quad (12)$$

$$M_{inc} = -\left(\bar{M}(I + pm_m^{-1}\delta_m)\right)^{-1}$$

where $\bar{M}$ is the mass nominal value, p_m is the uncertain values and δ_m is the amplitude of the uncertain $(-1 \leq \delta_m \leq 1)$. The matrix $\bar{M}^{-1}$ can be represented by a linear fraction transformation (LFT) in δ_m , like:

$$\bar{M} = \bar{M}^{-1}(I + pm_m^{-1}\delta_m)^{-1} = F_u(M_{mi}, \delta_m) \quad (13)$$

The block diagram of the Fig.5 shows how the uncertainty acts as a perturbation in the system interconnections.

The uncertain in this problem actuate in the matrices M. Than the uncertain amplitude is given by δ_m. One have 27 possibilities of δ_m, or else, we have 27 cases of uncertainties for each matrix M.

4 Simulations results

The main objective of the control in these simulations is stabilizing the tip mass angle (α) of the flexible link in a neutral position (0^o).

$$\alpha(t) = \arctan\left(\frac{w(x,t)}{L+R}\right) + \theta \quad (14)$$

When the tip comes to the neutral positions is important to see if the vibration was suppress, because

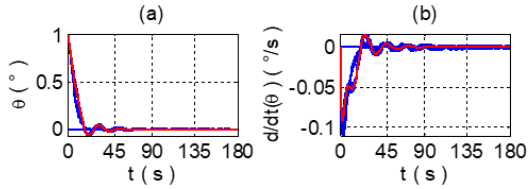

Figure 6: The angle θ and velocity $\dot{\theta}$, where red and blue lines are the nominal and the uncertainty cases

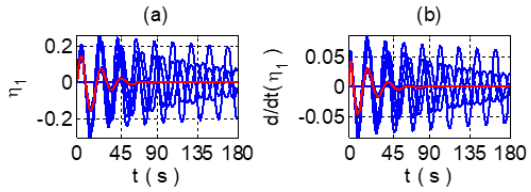

Figure 7: The flexible mode η_1 and velocity $\dot{\eta_1}$, where red and blue lines are the nominal and the uncertainty cases

with that we can assure that the control law design was robust enough to absorb the uncertainties and the vibrations do by the flexibility of the beam.

For the simulation it was considered the fallow values for the constant parameters: R = 0.05 m, bm = 0.15 m^2/s, Jrotor = 0.3 kgm^2, L = 1 m, ρ = 2700 kg/m, ke = 0.03, EI = 18.4 Nm^2, mtip = 0.25 kg and Jtip = 0.04 kgm^2.

One applies the H infinity control method for the 27 possible cases of uncertainty and the H_∞ controller gain for every case of uncertainty must be robust enough to control the flexible link in a time interval of 200 s and an initial condition $\theta = 1^o$.

4.1 Using the H_∞ control method

The Fig.6 shows that H∞ controller is able to control the rigid displacement θ (attitude) for the nominal case (red line: uncertainty zero) and for 16 cases of uncertainties (blue line) in less than 90 s. It is possible to see that some uncertainty cases the answer is better than the nominal case, showing that the influence of some parameters variation works to help the controller in the sense of minor overshoot and time rise.

The Fig.7 shows that H∞ controller is able to control the coordinate generalized of the first mode (η_1) and the variation rate of the first flexible mode ($\dot{\eta_1}$), for the nominal case (red line: uncertainty zero) and for 16 cases of uncertainties (blue line) in less than 100 s.

The Fig.8 shows that H∞ controller is able to control the coordinate generalized of the second mode (η_2) and the variation rate of the first flexible mode ($\dot{\eta_2}$),

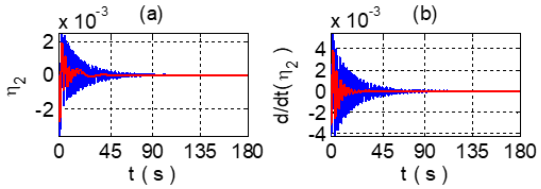

Figure 8: The flexible mode η_2 and velocity $\dot{\eta_2}$, where red and blue lines are the nominal and the uncertainty cases

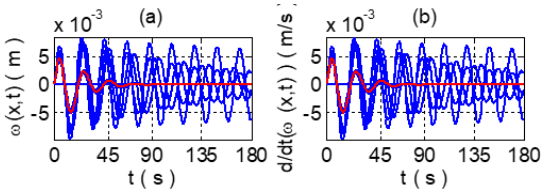

Figure 9: Comportment of the flexible displacement w(x, t) and his taxes variation

for the nominal case (red line: uncertainty zero) and for 16 cases of uncertainties (blue line) in less than 90 s.

In the Fig.9, shows the comportment of the flexible displacement w(xt) and his taxes variation, for the nominal case (red line: uncertainty zero) and for 16 cases of uncertainties (blue line), considering two vibrations modes. The maximum displacement was about 0.006 m.

Figure 10 show the H-infinity Energy spend (torque τ) to control the all 27 uncertainties cases (blue lines) where the red line is the nominal case. The response of the torque action shows that for 16 cases of uncertainties the system reach the equilibrium in less than 90 s with a maximum torque of 0.6 Nm.

Figure 11 show the angular position of the tip mass. The response of the evolution of the α angle shows that for 16 cases of uncertainties the system reach the equilibrium in less than 90 s. It is possible to see that some uncertainty cases the answer is better than

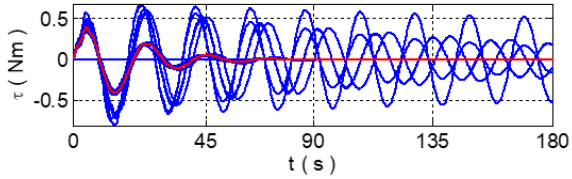

Figure 10: Response of the control effort τ, the red line is the nominal case and the blue lines are the uncertainty cases

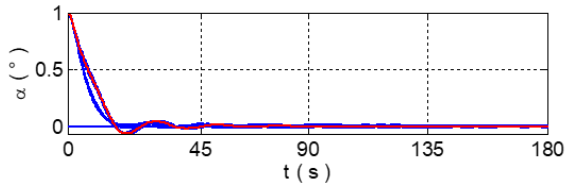

Figure 11: . Response of the angular position of the tip mass α, the red line is the nominal case and the blue lines are the uncertainty cases.

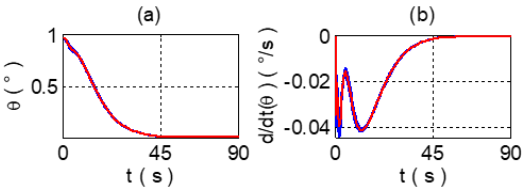

Figure 12: The angle θ and velocity $\dot{\theta}$, where red and blue lines are the nominal and the uncertainty cases

the nominal case, showing that the influence of some parameters variation works to help the controller in the sense of minor overshoot and time rise.

For 11 cases of uncertainties the H∞ method as not able to control, because this cases violates the boundary condition of this method.

4.2 Using the H∞/LMI control method

The Fig. 12 shows that H∞ method using a LMI pole allocation is able to control the rigid displacement θ (attitude) for the nominal case (red line: uncertainty zero) and for all 27 cases of uncertainties (blue line) in less than 50 s.

The Fig.13 shows that H∞ method using a LMI pole allocation is able to control the coordinate generalized of the first mode (η_1) and the variation rate of the first flexible mode ($\dot{\eta_1}$), for the nominal case (red line: uncertainty zero) and for all 27 cases of uncertainties (blue line) in less than 50 s

The Fig.14 shows that H∞ method using a LMI pole allocation is able to control the coordinate gen-

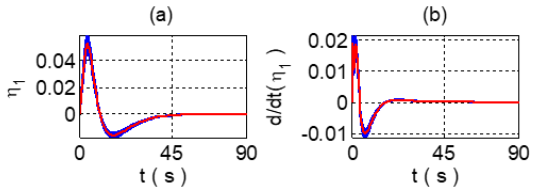

Figure 13: The flexible mode η_1 and rate ($\dot{\eta_1}$) - red and blue lines are the nominal and the uncertainty cases.

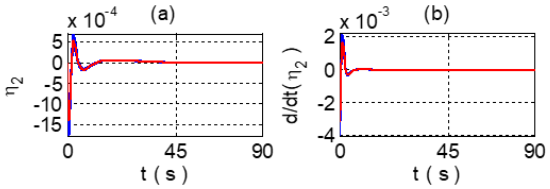

Figure 14: The flexible mode η_2 and rate ($\dot{\eta_2}$) - red and blue lines are the nominal and the uncertainty cases.

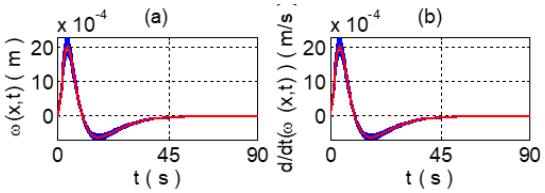

Figure 15: Comportment of the flexible deformation $w(x,t)$ and his taxes variation.

eralized of the second mode (η_2) and the variation rate of the second flexible mode ($\dot{\eta_2}$) for the nominal case (red line: uncertainty zero) and for all 27 cases of uncertainties (blue line) in less than 45 s.

In the Fig. 15, shows the comportment of the flexible displacement $w(x,t)$ and his taxes variation $\dot{w}(x,t)$, for the nominal case (red line: uncertainty zero) and for 16 cases of uncertainties (blue line), considering two vibrations modes. The maximum displacement was about 0.006 m.

Figure 16 show the H∞ Energy spend (torque τ) to control the all 27 uncertainties cases (blue lines) where the red line is the nominal case. The response of the torque action shows that for all 27 cases of uncertainties the system reach the equilibrium in less than 60 s with a maximum torque of 0.15 Nm.

Figure 17 show the angular position of the tip mass. The response of the evolution of the α angle shows that for all 27 cases of uncertainties the system reach the equilibrium in less than 60 s.

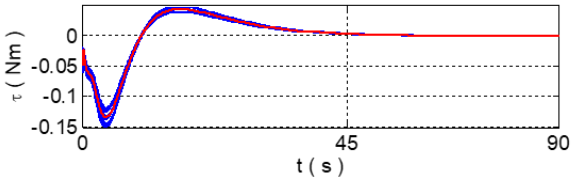

Figure 16: Response of the control effort τ, the red line is the nominal case and the blue lines are the uncertainty cases.

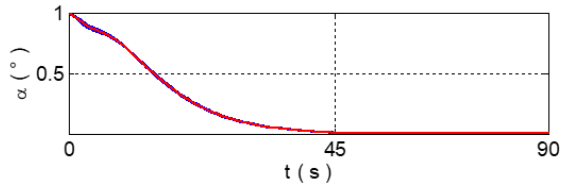

Figure 17: Response of the angular position of the tip mass α, the red line is the nominal case and the blue lines are the uncertainty cases.

4.3 Comparison between the two cases

From the set of figures presented it is very explicit that the performance of the control law design with the method H∞ with a LMI pole allocation was better, than the case were the control law was designed with only the H∞ method.

Comparing the Fig.6 and 12 (the angle rigid (θ) and his velocity ($\dot{\theta}$) it is verified that the variable was controlled in a shorter time (about 90 s) for the case with pole allocation (Fig.12). The Fig.7 and 13 (coordinate generalized of the first mode (η_1) and the variation rate of the first flexible mode ($\dot{\eta_1}$) it is verified that the variable was controlled in a shorter time (about 50 s) for the case with pole allocation (Fig.13). The Fig.8 and 14 (coordinate generalized of the second mode (η_2) and the variation rate of the second flexible mode ($\dot{\eta_2}$) it is verified that the variable was controlled in a shorter time (about 45 s) for the case with pole allocation (Fig. 14). The Fig. 9 and 15 (the angle rigid ($w(x,t)$) and his taxes variation ($\dot{w}(x,t)$) it can be seen that the maximum deflection generated in the case with pole allocation was lower than that obtained with the only H infinity method. The Fig.11 and 17 (the flexible angle (α)) has the same observations that make to the rigid angle. The Fig.10 and 16 shows the torque engenders, for the same task, the control law design with the H infinity with a LMI pole allocation was 25% less than that provided by the other method.

And for all cases the control law design with H ∞ LMI pole placement was able to control all cases of uncertainties. The possibility of region choice for the pole-assignment assures a better convergence of the H∞ algorithm. The region choice permit a control tuning more specific, in a sense of creates a frontier condition that restricting the existence of dominant poles ar from the axes of origin, and control the damping, overshoot and the distance of the natural frequencies. An important fact is these pole placement is done in the closed loop system, in a way to provides a satisfactory transient response.

5 Conclusion

This paper presents an attitude controller design for a rigid-flexible satellite comparing the performance between H∞ method considering and H∞ LMI pole placement with a parametrical uncertainty apply to the mass matrix.

The result of the simulations shows that the control laws designs, for the rigid flexible satellite, was able to support the parametric uncertainty and suppress the vibrations. The control law design with the H∞ with a LMI pole allocation was 25% less than that provided by the other method.

These results suggests that the controller design with the H∞ method with LMI pole allocation is more robust and efficient than the one provided by the H∞ method, due to the fact that of a better position of the closed loop system poles.

References:

[1] Romero, A. G. and Souza, L. C. G. , 2019 *State-dependent Riccati equation controller using Java in remote sensing CubeSats.* Journal of Applied Remote Sensing, v. 13, p. 1.

[2] Sidi, M. J, 1997. *Spacecraft dynamics and control: A practical engineering approach*. New York, NY: Cambridge University Press.

[3] Souza, S. G. and Souza, L. C. G, 2017. *Attitude Control System Design For A Rigid-Flexible Satellite Using The H-Infinity Method With Parametric Uncertainty*. Revista Interdisciplinar de Pesquisa em Engenharia, v. 2, p. 1-10.

[4] Murilo, A., de Deus Peixoto, P. J. , Souza, L. C. G. and Lopez, R. V. , 2021. *Real-time implementation of a parameterized Model Predictive Control for Attitude Control Systems of Rigid-flexible Satellite.* Mechanical systems and signal processing, v. 149, p. 107-129.

[5] Souza, A.G and Souza, L. C. G, 2015 *H infinity controller design to a rigid-flexible satellite with two vibration modes*, Journal of Physics: Conference Series, vol. 641, pp. 012030.

[6] Bigot, P.G., Souza, L. C. G. and SOUZA, A. G. *Application of Pareto Approach to Improve the State Dependent Ricatti Equation (SDRE) Controller Performance*. International Journal of Circuits, Systems and Signal Processing.

[7] Pinheiro, E.R. and Souza L.C.G, 2013. *Design of the Microsatellite Attitude Control System Using the Mixed H2/H∞ Method via LMI Optimization* Mathematical Problems in Engineering, vol. 2013, Article ID 257193, 8 pages. doi:10.1155/2013/25719.

[8] Gasbarri P., Monti R., De Angelis C. and Sabatini M., 2014. *Effects of uncertainties and flexible dynamic contributions on the control of a spacecraft full-coupled model*, Acta Astronautics, Volume 94, Issue 1, January–February 2014, Pages 515-526, ISSN 0094-5765, http://dx.doi.org/10.1016/j.actaastro.2012.08.018.

[9] H. C. Ferreira, R. S. Baptista, J. Y. Ishihara and G. A. Borges, 2011. *Disturbance rejection in a fixed wing UAV using nonlinear H∞ state feedback*, 2011 9th IEEE International Conference on Control and Automation (ICCA), Santiago, pp. 386-391.

[10] Chilali, M. Gahinet and Apkarian P., 1999. *Robust pole placement in LMI regions*. IEEE Transactions on automatic control, v. 44, n. 12, p. 2257 – 2270.

[11] Junkins, J. L and Kim, 1993. Y. *Introduction to dynamics and control of flexible structures*. Washington, DC: American Institute of Aeronautics and Astronautics (AIAA).

[12] Zhou, K and Doyle, J. C, *Essentials of robust control*. Upper Saddle River, NJ: Prentice-Hall, 1998.

[13] Skogestad, S, Postlethwaite, I, 2001. *Multivariable feedback control: analysis and design*. Chichester, UK: John Wiley and Sons.

[14] Gu D.W., Petkov P.H. and Konstantinov M.M, 2005. *Robust control design, with matlab*, London, UK Springer.

Contribution of individual authors to the creation of a scientific article (ghostwriting policy)

Alain G de Souza and Luiz C G de Souza carried out the modeling, simulation and ACS design.

Follow: www.wseas.org/multimedia/contributor-role-instruction.pdf

Sources of funding for research presented in a scientific article or scientific article itself

The authors are grateful for the funding of coordination of improvement of higher-level personnel (Coordenação de Aperfeiçoamento de Pessoal de Nível Superior - CAPES) and the National Institute for Space Research (Instituto Nacional de Pesquisas Espaciais - INPE), for the facilities.